JPn Neuroscience

The Journal of Physiology

J Physiol 591.1 (2013) pp 365–378

Activation of metabotropic glutamate receptors improves the accuracy of coincidence detection by presynaptic mechanisms in the nucleus laminaris of the chick

Hiroko Okuda[1], Rei Yamada[2], Hiroshi Kuba[2,3] and Harunori Ohmori[1]

[1] *Department of Physiology, Faculty of Medicine, Kyoto University, Yoshida-Konoe-cho, Sakyo-ku, Kyoto 606-8501, Japan*
[2] *Department of Cell Physiology, Nagoya University Graduate School of Medicine, 65 Tsurumai-cho, Showa-ku, Nagoya 466-8550, Japan*
[3] *PRESTO, JST, Saitama 332-0012, Japan*

Key points

- Interaural time difference (ITD) is a major cue for sound source localization and is processed by detecting a coincidence of bilateral excitatory postsynaptic potentials (EPSPs) in the nucleus laminaris (NL) in birds.
- The sharpness of coincidence detection (CD) depends on the speed and size of EPSPs. We found here a regulatory mechanism of EPSP size through the presynaptic mGluR activity.
- The activation of mGluRs reduced the transmitter release and extent of excitatory postsynaptic current depression during tetanic stimulation, but improved the CD. Furthermore, the activity of mGluRs and their expression were graded along the tonotopic axis and were stronger toward the low frequency neurons of NL.
- We proposed an idea that the presynaptic mGluRs may operate as a self-regulatory mechanism to optimize the size of EPSP and have roles in sharpening the CD. This regulatory mechanism may underlie the sound source localization particularly during a long-lasting sound in the NL.

Abstract Interaural time difference (ITD) is a major cue for localizing a sound source and is processed in the nucleus laminaris (NL) in birds. Coincidence detection (CD) is a crucial step for processing ITD and critically depends on the size and time course of excitatory postsynaptic potentials (EPSPs). Here, we investigated a role of metabotropic glutamate receptors (mGluRs) in the regulation of EPSP amplitude and CD in the NL of chicks. A non-specific agonist of mGluRs ((±)-1-aminocyclopentane-*trans*-1,3-dicarboxylic acid; t-ACPD) reduced the amplitude and extent of depression of excitatory postsynaptic currents (EPSCs) during a stimulus train, while the paired pulse ratio and coefficient of variation of EPSC amplitude were increased. In contrast, the amplitudes of spontaneous EPSCs were not affected, but the frequency was reduced. Thus, the effects of t-ACPD were presynaptic and reduced the release of neurotransmitter from terminals in the NL. Expression of group II mGluRs was graded along the tonotopic axis and was stronger towards the low frequency region in the NL. Both group II (DCG-IV) and group III (L-AP4) specific agonists reduced EPSC amplitude by presynaptic mechanisms, and the reduction was larger in the low frequency region; however, we could not find any effects of group I-specific agonists on EPSCs. The reduced EPSP amplitude in DCG-IV improved CD. A specific antagonist of group II mGluRs (LY341495) increased the amplitude of both EPSCs and EPSPs and enhanced the depression during a stimulus train, indicating constitutive activation of mGluRs in the NL.

DOI: 10.1113/jphysiol.2012.244350

These observations indicate that mGluRs may work as autoreceptors and regulate EPSP size to improve CD in the NL.

(Resubmitted 6 September 2012; accepted after revision 22 October 2012; first published online 22 October 2012)
Corresponding author H. Okuda: Department of Physiology, Faculty of Medicine, Kyoto University, Yoshida-Konoe-cho, Sakyo-ku, Kyoto 606-8501, Japan. Email: okuda@nbiol.med.kyoto-u.ac.jp

Abbreviations CD, coincidence detection; CF, characteristic frequency; CV, coefficient of variation; DCG-IV, (2*S*,2′*R*,3′*R*)-2-(2′,3′dicarboxycyclopropyl)glycine; DHPG, 3,5-dihydroxyphenylglycine; HCN, hyperpolarization-activated and cyclic nucleotide-gated; ITD, interaural time difference; L-AP4, L-(+)-2-amino-4-phosphonobutyric acid; mGluR, metabotropic glutamate receptor; MNTB, medial nucleus of the trapezoid body; NL, nucleus laminaris; NM, nucleus magnocellularis; PPR, paired pulse ratio; ROI, regions of interest; sEPSC, spontaneous EPSC; t-ACPD, (±)-1-aminocyclopentane-*trans*-1,3-dicarboxylic acid; VGluT2, vesicular glutamate transporter 2.

Introduction

Interaural time difference (ITD) is one of the critical cues for sound source localization (Klumpp & Eady, 1956; Carr & Konishi, 1990; Yin & Chan, 1990). In birds, the nucleus laminaris (NL) detects the coincidence of excitatory synaptic inputs from the bilateral nucleus magnocellularis (NM) and processes the ITD (Park & Rubel, 1975). The accuracy of coincidence detection (CD) depends on the time course and amplitude of excitatory postsynaptic potential (EPSPs) (Reyes *et al.* 1996; Kuba *et al.* 2002*a*, 2003). The fast kinetics and small size of EPSPs narrow the time window to trigger spikes by the coincidence of bilateral EPSPs, and hence improve CD in the NL. The decay time course of EPSPs in the NL is determined mostly by activation of the low-voltage-activated K^+ channel Kv1.2 (Kuba *et al.* 2005). The amplitudes of EPSPs decrease with the progress of synaptic depression in a stimulus train and improve CD (Kuba *et al.* 2002*a*; Cook *et al.* 2003). However, small subthreshold EPSPs are not able to trigger spikes (Kuba *et al.* 2002*a*); thus, it is ideal to have a mechanism to optimize the size of EPSPs during ongoing stimuli.

In nuclei of the auditory brainstem of mammals and avians, several different types of presynaptic receptors are known to regulate transmitter release by modulating calcium and potassium currents (Barnes-Davies & Forsythe, 1995; Lachica *et al.* 1995; Otis & Trussell, 1996; Takahashi *et al.* 1996, 1998; Leao & von Gersdorff, 2002). Metabotropic glutamate receptors (mGluRs) are known to work as autoreceptors at glutamatergic presynaptic terminals and depress the release of neurotransmitter (Conn & Pin, 1997). In the presynaptic terminal to the medial nucleus of the trapezoid body (MNTB) of rats, group II (mGluRs 2, 3) and group III (mGluRs 4, 6–8) mGluRs are negatively coupled to the transmitter release mechanism (Barnes-Davies & Forsythe, 1995; von Gersdorff *et al.* 1997). In chicken embryos, GABAergic transmission was suppressed by activation of mGluRs both in the NM and the NL (Lu, 2007; Tang *et al.* 2009); however, glutamatergic transmission was not affected in the NL. Because both neuronal activity and the synaptic transmission change greatly after hatching (Kuba *et al.* 2002*a*,*b*), we examined the modulatory roles of mGluRs in the NL of post-hatch chicken and found that mGluRs decreased the size of EPSPs and improved the CD.

Methods

Slice preparations

Animals were kept and used according to the regulations of the Animal Research Committee, Graduate School of Medicine, Kyoto University. Brain slices were prepared from chickens (*Gallus domesticus*) aged from 1 to 4 post-hatch days (P1–P4) for electrophysiological experiments. The numbers of animals used were as follows: post-hatch day/number, P1/34, P2/17, P3/20 and P4/1. Detailed procedures of brain slice preparation are described in a previous paper (Kuba *et al.* 2003).

Electrophysiological recordings

Whole cell recordings were made with a patch-clamp amplifier (EPC-8; HEKA Elektronik, Lambrecht, Germany). Patch pipettes were fabricated from thin-walled borosilicate glass capillaries (GC150TF-100, Harvard, MA, USA) and had a resistance of 2–5 MΩ when filled with a KCl-based internal solution (in mM: 160 KCl, 0.2 EGTA and 10 Hepes–KOH, pH 7.4). Pipettes were coated with a silicone resin (Sylgard 184; Dow Corning Asia, Tokyo, Japan) and tips were fire polished before use. Electrode capacitance was compensated electrically, and series resistance was less than 13 MΩ and compensated by 60–80%. If the series resistance changed more than 25% during recordings, the cell was excluded from analysis. The liquid junction potential (−3 mV) was corrected. During experiments, slices were continuously perfused with normal artificial cerebrospinal fluid (ACSF) (in mM: 125 NaCl, 2.5 KCl, 26 $NaHCO_3$, 1.25 NaH_2PO_4, 3 $CaCl_2$, 1 $MgCl_2$, 17 glucose, pH 7.4, 320–330 mosmol). In this study, Ca^{2+} concentration of the extracellular medium

was 3 mM to make the effects of mGluRs clear unless otherwise stated (Maki *et al.* 1990; Zhang & Trussell, 1994). All experiments were performed at 40°C.

The resting membrane potential was measured immediately after the whole cell recording configuration was achieved. $GABA_A$ receptors were blocked by bicuculline (40 μM, Tocris, Bristol, UK). Electrical stimulation was applied every 10 s through a bipolar tungsten electrode to projection fibres from either the ipsilateral or contralateral NM as described previously (Kuba *et al.* 2002*a*; see also Fig. 1*A*). A train of stimulation or pulse pairs were applied at 3–10 ms inter-pulse intervals. Spontaneous excitatory postsynaptic currents (sEPSCs) were recorded at −83 mV. In experiments to evaluate CD (Fig. 8), a train of four stimuli at 10 ms intervals was applied while changing the time separation (Δt, 0–1 ms) between the ipsilateral and contralateral electrical stimulation in 0.2 ms steps. Contralateral leading and ipsilateral leading stimuli were not distinguished in the analysis, and the firing probability was plotted as a function of absolute value of Δt (Fig. 8*D*). Spikes were confirmed by the time derivative of the voltage records. Firing probability, defined as the number of spikes divided by the total number of stimuli, was calculated at each Δt from eight to 32 records. The stimulus intensity was tuned at the beginning of each experiment so that unilateral stimuli alone did not trigger a spike. Once set, the stimulus intensity was maintained throughout the experiment (Joseph & Hyson, 1993; Kuba *et al.* 2002*b*).

3,5-Dihydroxyphenylglycine (DHPG; a selective agonist of group I mGluRs, 40 μM, Tocris), (±)-1-amino-cyclopentane-*trans*-1,3-dicarboxylic acid (t-ACPD, group I and group II mGluR agonist, 100 μM, Tocris), (2*S*,2′*R*, 3′*R*)-2-(2′,3′dicarboxycyclopropyl)glycine (DCG-IV, a selective agonist of group II mGluRs, 1–5 μM, Tocris), LY341495 (a selective antagonist of group II mGluRs, 0.2 μM, Tocris) or L-(+)-2-amino-4-phosphonobutyric acid (L-AP4, a selective agonist of group III mGluRs, 100 μM, Wako, Osaka, Japan) was bath applied. Concentrations of these drugs followed preceding studies (Barnes-Davies & Forsythe, 1995; Takahashi *et al.* 1996; Lu, 2007; Nishimaki *et al.* 2007). Measurements were taken at least 3 min after the application of drugs.

Data acquisition and analysis

Voltage and current output signals from the patch-clamp amplifier were filtered at 5 kHz through a four-pole low-pass filter with Bessel characteristics (UF-BL2; NF Corp., Yokohama, Japan) and sampled at 10–50 kHz by a 12-bit analog-to-digital converter (ADM-8298BPC, Micro Science, Tokyo, Japan) with an in-house data acquisition program. Off-line analysis was conducted with commercially available software (Axograph; Axon Instruments, Union City, CA, USA). The coefficient of variation (CV) of EPSC amplitudes (Korn & Faber, 1991; Manabe *et al.* 1993) and paired pulse ratio (PPR; EPSC2/EPSC1) were calculated from five to 20 traces. The inter-event interval and the amplitude of the sEPSCs were calculated from 15 to 45 events in each cell. Data are given as the means ± S.E.M. Statistical significance was tested with Student's paired *t* test unless otherwise stated.

Immunohistochemistry

Nine embryos (E18, six; E21, three) and 22 post-hatch chicks (P2, four; P3, two; P4, five; P5, seven; P6, three; P16, one) were used for immunohistochemistry. Detailed procedures are described in a previous paper (Kuba *et al.* 2005). The antibodies to mGluR subtypes (mGluR1–5, 7 and 8) were as follows: anti-human-mGluR1 rabbit polyclonal antibody (Stressgen, Brussels, Belgium), anti-mGluR2/3 rabbit polyclonal antibody (Merck Millipore, Billerica, MA, USA), anti-mGluR4 rabbit polyclonal antibody (MBL), anti-mGluR5 rabbit polyclonal antibody (Merck Millipore), anti-human-mGluR7 mouse monoclonal antibody (Research Biochemicals, Cleveland, UK) and anti-mGluR8 guinea pig polyclonal antibody (Merck Millipore). These antibodies had homologies with the chick database (NCBI, Bethesda, MD, USA) of more than 90% for mGluR1, 5, 7 and 8 and 87% for mGluR2/3. Despite the lack of an mGluR4 database for the chick, a homology of more than 85% was confirmed with the zebra finch (*Taeniopygia guttata*) (Wada *et al.* 2004). mGluR6 was not tested because its expression is limited to the mammalian retina (Nakajima *et al.* 1993). For visualization, Alexa488-conjugated anti-rabbit, anti-mouse or anti-guinea pig IgG (Molecular Probes, Carlsbad, CA, USA) was used. Slices were mounted on to glass slides, coverslipped and observed under a confocal laser-scanning microscope (FV1000, Olympus). Reactivity of the antibodies was confirmed as positive in chick cerebellum ($n = 3$ for each antibody) against Purkinje cells for mGluR1 and mGluR7 and Golgi cells for mGluR2/3 and mGluR5 (Phillips *et al.* 1998; Ferraguti & Shigemoto, 2006). However, the reactivities of mGluR4 and mGluR8 antibodies were negative in chick cerebellum and hippocampus, respectively (Corti *et al.* 1998, 2002). Thus, we did not examine the immunoreactivity of mGluR4 or mGluR8 in the NL region.

The immunoreactivity of NL neurons was measured quantitatively by setting regions of interest (ROI; 10×10 μm) in the bilateral dendritic area of the NL neurons using ImageJ, NIH, Bethesda, CA, USA and the intensity was normalized relative to the intensity measured in the medial vestibular nucleus in the same slice. Immunoreactivity was compared among the following three characteristic frequency (CF) regions (Fig. 3*B*) that follow a previous definition (Rubel & Parks, 1975; Kuba *et al.* 2005): high-CF region (>2.5 kHz, sectors

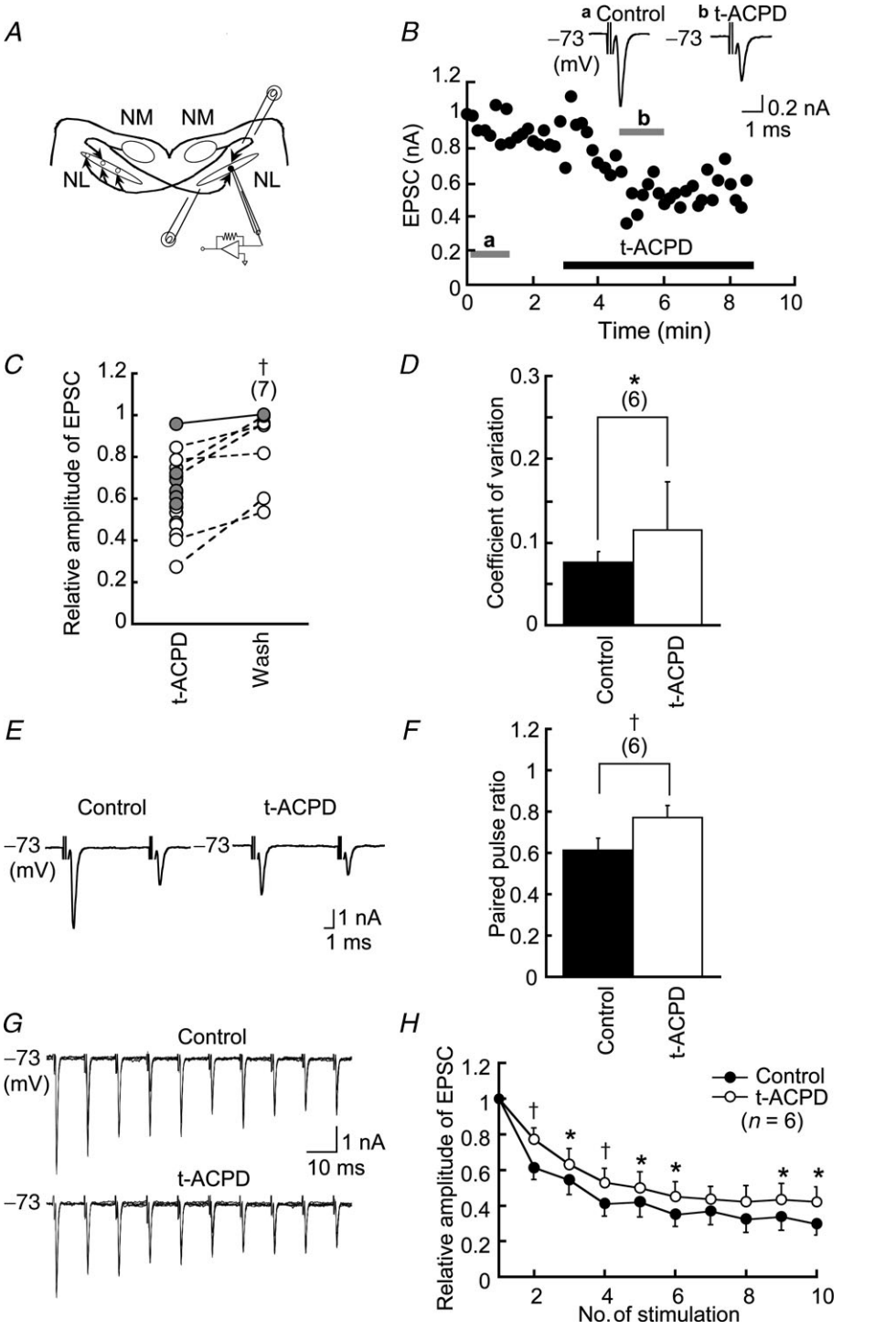

Figure 1. Effects of t-ACPD on EPSCs
A, schematic diagram of the interaural time difference coding circuit in the avian auditory brainstem. *B*, EPSC amplitude was reduced by bath-applied t-ACPD and was partially recovered by wash; EPSCs were induced every 10 s. Inset 2 traces show the average EPSC in bars at *a* and *b*. *C*, relative amplitude of EPSC to the control in t-ACPD and 4 min after washout of t-ACPD ($n = 7$). Filled circles and a continuous line indicate experiments in 3 mM Ca^{2+} and open circles and dashed lines in 2 mM Ca^{2+} in the extracellular medium. Connected points were recorded in the same neurons. *D*, t-ACPD increased the coefficient of variation of EPSC amplitude ($n = 6$). *E*, paired pulse records of EPSCs; ensemble averages of seven to 10 consecutive traces. *F*, t-ACPD increased the paired pulse ratio ($n = 6$). *G*, EPSCs generated by a train of 10 pulses; superposed of five consecutive traces. *H*, amplitudes of EPSCs in the train relative to the first EPSC in the train. Depression

1–4), middle-CF region (1–2.5 kHz, sectors 5–8) and low-CF region (<1 kHz, sectors 9–11). In some slices, anti-mGluR2/3 antibody was double-immunostained with anti-Kv1.2 antibody (mouse monoclonal IgG; Merck Millipore) to measure the cell number or anti-vesicular glutamate transporter 2 (anti-VGluT2) antibody (mouse monoclonal IgG; NeuroMab, Davis, CA, USA) to evaluate the density of excitatory synapses. Cell numbers within an ROI were counted by visual inspection.

Results

The metabotropic glutamate receptor agonist t-ACPD reduced the amplitude of excitatory postsynaptic currents

We examined whether the non-specific mGluR agonist t-ACPD affected the amplitude of EPSCs in middle-CF neurons of the NL, where CD was most accurate (Kuba *et al.* 2005). EPSCs were recorded at −73 mV by stimulating either the ipsilateral or contralateral projection fibres from the NM (Fig. 1*A*). EPSC amplitudes were reduced by application of t-ACPD (100 μM) in all neurons tested (2.09 ± 0.69 nA in the control and 1.41 ± 0.45 nA in t-ACPD, $n = 6$, $P < 0.05$, Student's paired *t* test) and partially recovered after wash (Fig. 1*C*). We assessed whether the effect of t-ACPD was of pre- or postsynaptic origin. Both the CV and PPR of EPSC amplitudes increased after application of t-ACPD; the CV increased by a factor of 1.56 (Fig. 1*D*, $n = 6$, $P < 0.05$), and the PPR increased by a factor of 1.23 (Fig. 1*E* and *F*; $n = 6$, $P < 0.01$). The amplitude of sEPSCs was not changed by t-ACPD (Fig. 2*A*), whereas the inter-event interval was prolonged (Fig. 2*B*). Thus, t-ACPD likely reduces the EPSC amplitude by reducing transmitter release presynaptically. During a train of 10 pulses delivered at 10 ms inter-pulse intervals, the EPSC amplitude was depressed both in control and t-ACPD conditions (Fig. 1*G* and *H*); however, the rate of depression was slower, and the extent was smaller, in t-ACPD (Fig. 1*H*). When measured by fitting a single exponential function, the time course of EPSC depression was 15.67 ± 2.03 ms in the control and 21.53 ± 1.64 ms in t-ACPD ($n = 6$, $P < 0.05$), and the relative amplitude of the 10th EPSC compared to the first one increased; 0.28 ± 0.05 in the control and 0.37 ± 0.08 in t-ACPD ($n = 6$, $P < 0.05$). These results indicate that activation of presynaptic mGluRs reduced transmitter release and prevented depression during the repetitive stimuli of NL.

We further compared the probabilistic nature of synaptic transmission in 2 and 3 mM Ca^{2+} concentrations and the t-ACPD effects on them, because in previous experiments we used 2 mM Ca^{2+} ACSF as a standard extracellular medium (see Methods). There was no significant difference between them in the amplitude of the first EPSC in a train, CV of the EPSC amplitudes and the PPR ($P > 0.05$, unpaired Student's *t* test; $n = 14$ for 2 mM Ca^{2+} ACSF; $n = 6$ for 3 mM Ca^{2+} ACSF) and no differences either in t-ACPD effects (t-ACPD/control, $P > 0.05$, unpaired Student's *t* test; $n = 14$ for 2 mM Ca^{2+} ACSF; $n = 6$ for 3 mM Ca^{2+} ACSF).

The t-ACPD effects on the amplitude of sEPSCs and inter-event interval were similarly observed in 2 mM Ca^{2+} concentrations ($n = 6$). t-ACPD similarly reduced the rate of depression of EPSC amplitude during a train in 2 mM Ca^{2+} ACSF; decay time constant was 17.34 ± 1.19 ms in the control and 23.11 ± 1.68 ms in t-ACPD ($n = 12$, $P < 0.01$), and the relative amplitude of 10th EPSC to the first EPSC increased ($n = 12$, $P < 0.01$). These results indicate that these t-ACPD effects were not different between 2 and 3 mM Ca^{2+} ACSF.

Expression of metabotropic glutamate receptor 2/3 along the tonotopic axis

We examined the expression pattern of mGluR subtypes in the NL with immunohistochemistry. Marked expression of mGluR2/3 (group II mGluRs) was found in the low-CF region, particularly in the dendritic areas (Fig. 3*A*). For group I mGluRs, the immunoreactivity to mGluR5 antibody was not evident in the NL, whereas slight reactivity was found for mGluR1 in a restricted dendritic region of low-CF NL (caudo-lateral edge of NL of P5 chick, data not shown). Immunoreactivity to group III mGluR antibody was examined only for mGluR7 (see Methods) and was negligible in the NL region (data not shown). Thus, we measured the expression level of mGluR2/3 quantitatively across CF regions (see Methods). Expression was significantly higher in the low-CF regions (Fig. 3*C*; $n = 15$, $P < 0.01$; high-CF = 1.22 ± 0.05, middle-CF = 1.75 ± 0.05, low-CF = 3.03 ± 0.11). Although the immunological density might have been affected by the difference in cell densities in different CF regions of the NL, even after correcting for number of cells in each CF region (see Methods), the expression level of mGluR2/3 was still high in the low-CF region (1.19 in the middle-CF

progressed with a time constant of 15.67 ± 2.03 ms in the control and 21.53 ± 1.64 ms in t-ACPD ($n = 6$). *$P < 0.05$; †$P < 0.01$. Here and in subsequent figures, the numbers in parentheses indicate the number of cells. EPSC, excitatory postsynaptic current; NL, nucleus laminaris; NM, nucleus magnocellularis; t-ACPD, (±)-1-aminocyclopentane-*trans*-1,3-dicarboxylic acid.

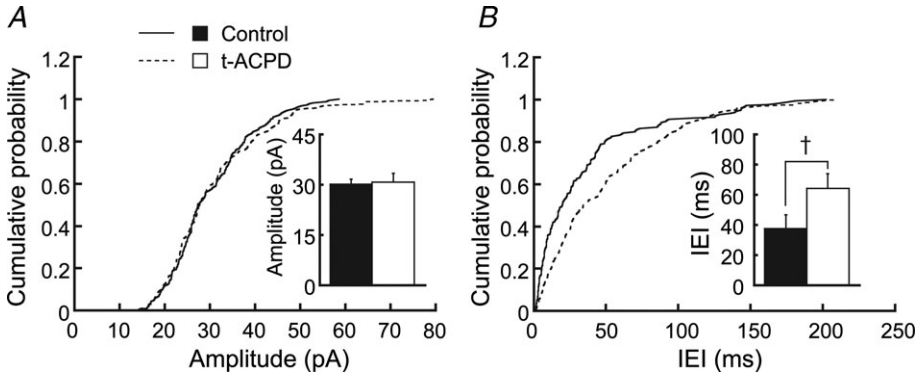

Figure 2. Effects of t-ACPD on sEPSCs
sEPSCs were recorded at −83 mV in artificial cerebrospinal fluid with bicuculline (40 μM). t-ACPD prolonged the IEI but did not affect the amplitude of sEPSCs ($n = 189$ control events and 174 in t-ACPD). *A* and *B* are the cumulative distribution of amplitudes and IEIs of sEPSCs, respectively. Bar graphs show averages in the control and after 3 min in t-ACPD. The difference was significant for IEI ($n = 5$, Kolmogorov–Smirnov test, $P < 0.01$). IEI, inter-event interval; sEPSC, spontaneous excitatory postsynaptic current; t-ACPD, (±)-1-aminocyclopentane-*trans*-1,3-dicarboxylic acid. †$P < 0.01$.

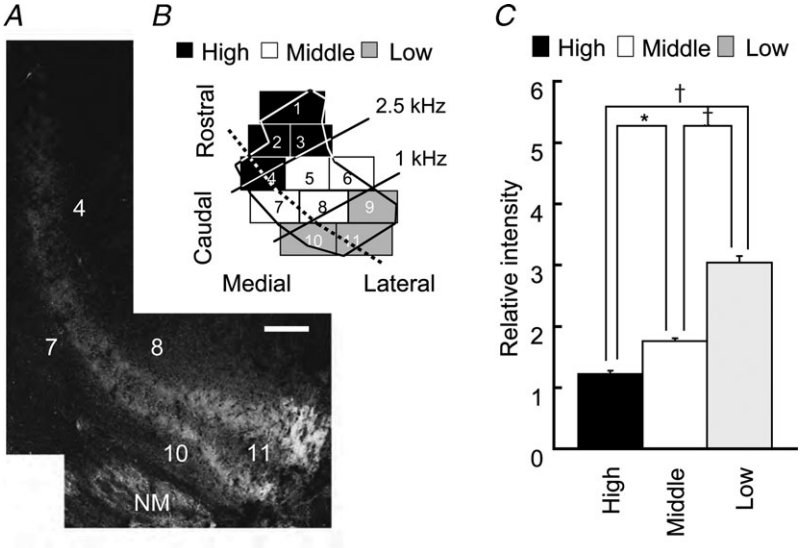

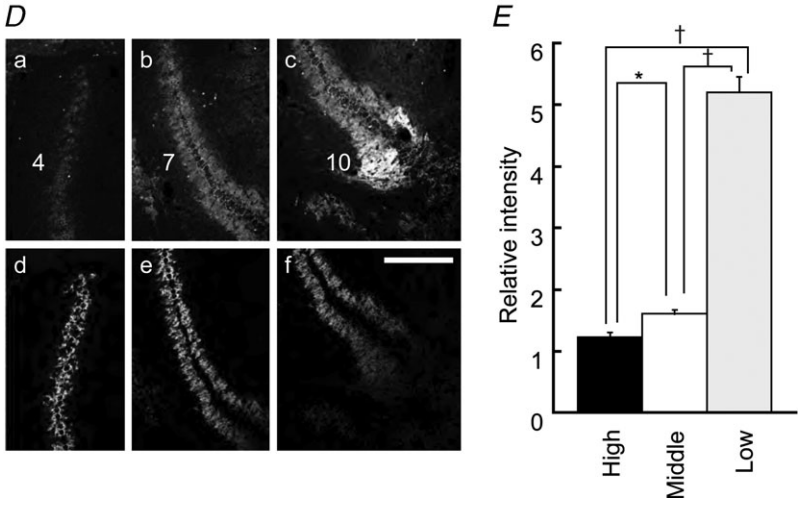

Figure 3. Immunohistochemistry of mGluR2/3
A, fluorescence image from a slice containing the three CF regions of the NL along the broken line in *B*. Numbers correspond to sectors labelled in *B*. *B*, a scheme of two-dimensional projections of the NL. *C*, immunopositivity for mGluR2/3 relative to the medial vestibular nucleus is plotted for the three CF regions of the NL. Data from 15 chicks were averaged. *D*, double-immunostaining for mGluR2/3 (*a*–c) and VGluT2 (*d*–*f*) in the three CF regions. *E*, the intensity of mGluR2/3 to the expression level of VGluT2 among the three CF regions of the NL. Data from nine chicks were averaged. Scale bar is 100 μm. *A* and *D* are different slices. CF, characteristic frequency; mGluR, metabotropic glutamate receptor; NL, nucleus laminaris; NM, nucleus magnocellularis; VGluT2, vesicular glutamate transporter 2. *$P < 0.05$ and †$P < 0.01$.

region and 1.53 in the low-CF region, relative to the high-CF region). Cell densities in ROIs were 1.28 in the middle-CF region and 1.51 in the low-CF region, relative to the high-CF region. Furthermore, the low-CF NL neurons have long primary dendrites that branch extensively and may affect the density of presynaptic terminals (Kuba *et al.* 2005). Therefore, we assessed the synaptic density with VGluT2 immunoreactivity (Fig. 3*Dd–f*). The VGluT2 immunoreactivity was lowest in the low-CF region and highest in the middle-CF region (1.09 in the middle-CF and 0.56 in the low-CF region, relative to the expression level in the high-CF region, $n = 9$). When expression levels of mGluR2/3 (Fig. 3*Da–c*) were normalized by the expression level of VGluT2 (Fig. 3*Dd–f*), the relative expression of mGluR2/3 was particularly high in the low-CF NL region (high-CF $= 1.22 \pm 0.08$, middle-CF $= 1.60 \pm 0.07$, low-CF $= 5.20 \pm 0.25$, Fig. 3*E*; $n = 9$, $P < 0.05$).

We further examined the expression of mGluR2/3 during the development of the animal (Fig. 4) and found that the expression was low in embryonic chicks and increased greatly after the hatch (Fig. 4*C*; $P < 0.01$); this increase was apparent particularly in the dendritic region of low-CF NL neurons (Fig. 4*A* and *B*). After the hatch, the relative expression of mGluR2/3 was not different between P2 and P5 (Fig. 4*C*; high-CF $P > 0.69$, middle-CF $P > 0.56$, low-CF $P > 0.87$).

Effects of specific agonists on excitatory postsynaptic currents

Because mGluR2/3 is expressed in the NL and the expression is graded towards the low-CF region, we compared the effects of a specific agonist of mGluR2/3 (DCG-IV, 5 μM group II mGluRs agonist) between high- and low-CF neurons. Here we tested DCG-IV effects on EPSCs in 2 mM Ca^{2+} extracellular medium because we do not have a complete data set to test the statistics of transmission in the 3 mM Ca^{2+} medium. In the 3 mM Ca^{2+} extracellular medium, DCG-IV (1 μM) still suppressed the EPSC amplitude to 0.51 ± 0.18 ($n = 7$) of the control in the low-CF neurons. Figure 5*A* shows EPSCs generated by a pair of stimuli applied at a 3 ms inter-pulse interval. DCG-IV reduced the amplitude of the first EPSC. However, the reduction was larger in the low-CF NL neurons (Fig. 5*B* and Table 1). The first EPSCs were reduced by a factor of 0.75 and 0.39 of the control in the high-CF and low-CF neurons, respectively. In the high-CF neurons, neither the CV of the first EPSC nor the PPR were significantly affected by DCG-IV, while the CV and PPR in the low-CF neurons increased by a factor of 2.09 and 1.32 of the control, respectively (Fig. 5*C* and *D*, Table 1). It should be noted that EPSCs in the middle-CF neurons were similarly affected by DCG-IV, and the effects were closer to those on the low-CF neurons (Table 1). These results indicate that activation of group II mGluRs reduced synaptic transmission, and the extent of this reduction was frequency–region-dependent and larger towards the low-CF region. Moreover, the suppressive effects of DCG-IV (5 μM) on EPSCs were counteracted by a group II mGluR antagonist (LY341495 0.2 μM) in the low-CF NL neurons: the first EPSC was 1.36 ± 0.41 nA in LY341495 and 1.35 ± 0.41 nA in LY341495 plus DCG-IV ($P > 0.87$, $n = 3$).

We further examined the effects of other groups of mGluRs. In the presence of DCG-IV, application of a

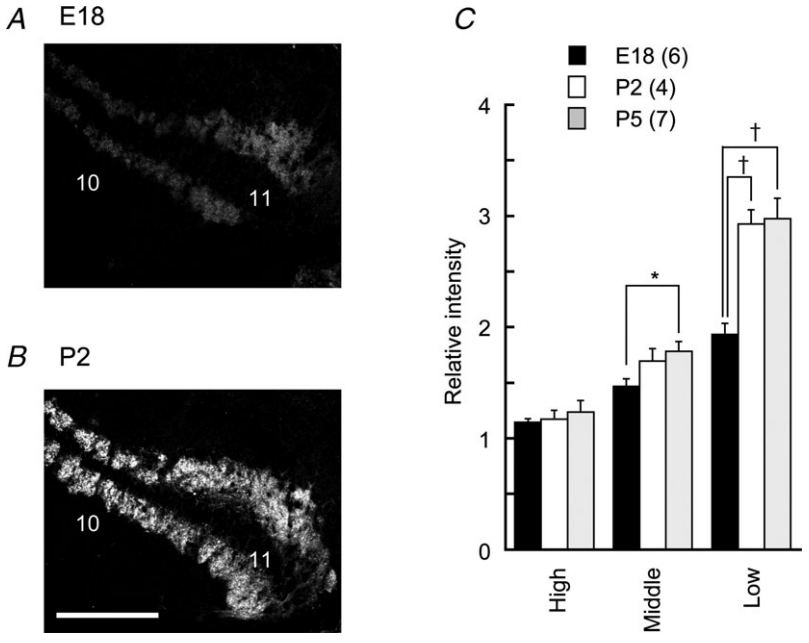

Figure 4. Immunostaining for mGluR 2/3 increased with development
Immunostaining for mGluR2/3 in the low-CF region of the NL at E18 (*A*), P2 (*B*). *C*, expression of mGluR2/3 between the three CF regions and comparison of the mature and immature NL. Scale bar is 100 μm. E, embryo day; P, post-hatch day; CF, characteristic frequency. †$P < 0.01$.

Table 1. Effects of group II and group III agonists on EPSCs in the three CF regions of the nucleus laminaris

					In the presence of DCG-IV		
CF region		Control	DCG-IV	DCG-IV/ Control	Control	L-AP4	L-AP4/ Control
High	Amplitude of 1st EPSC (nA)	2.25 ± 0.82 (6)	1.69 ± 0.69 (6)*	0.75	2.64 ± 0.62 (4)	2.28 ± 0.65 (4)	0.87
	CV	0.09 ± 0.02 (6)	0.12 ± 0.02 (6)	1.31	0.08 ± 0.01 (4)	0.09 ± 0.01 (4)	1.05
	PPR	0.89 ± 0.12 (3)	0.88 ± 0.09 (3)	0.98	0.58 ± 0.04 (4)	0.68 ± 0.03 (4)	1.16
Middle	Amplitude of 1st EPSC (nA)	1.35 ± 0.46 (6)	0.75 ± 0.29 (6)*	0.56	2.48 ± 0.52 (4)	1.68 ± 0.43 (4)*	0.68
	CV	0.11 ± 0.02 (5)	0.15 ± 0.03 (5)*	1.44	0.12 ± 0.05 (4)	0.18 ± 0.07 (4)*	1.57
	PPR	0.55 ± 0.18 (3)	0.77 ± 0.18 (3)*	1.39	0.67 ± 0.16 (4)	0.90 ± 0.14 (4)	1.34
Low	Amplitude of 1st EPSC (nA)	2.31 ± 0.44 (6)	0.91 ± 0.18 (6)†	0.39	2.01 ± 0.72 (5)	1.18 ± 0.48 (5)*	0.58
	CV	0.09 ± 0.02 (6)	0.18 ± 0.03 (6)†	2.09	0.14 ± 0.03 (5)	0.20 ± 0.04 (5)*	1.49
	PPR	0.70 ± 0.06 (6)	0.93 ± 0.05 (6)†	1.32	0.91 ± 0.10 (5)	1.24 ± 0.15 (5)*	1.37

The effect of L-AP4 was examined in the presence of DCG-IV. CF, characteristic frequency; CV, coefficient of variation; EPSC, excitatory postsynaptic current; PPR, paired pulse ratio. *$P < 0.05$; †$P < 0.01$. The number of cells is indicated in parentheses.

group III selective agonist (L-AP4, 100 μM) further reduced EPSC amplitudes, and both the CV and PPR were increased in the middle- to low-CF neurons (Table 1; $P < 0.05$). In the high-CF neurons, the EPSC amplitudes, CV and PPR were not significantly affected by L-AP4 ($P > 0.06$, $n = 4$). The group I agonist DHPG (40 μM) did not affect the PPR of EPSCs in the presence of DCG-IV ($P > 0.88$, $n = 4$, data not shown). Thus, group II and group III mGluRs are most likely negatively coupled with transmitter release in the middle- to low-CF NL neurons. Although, the antibodies used may not have been appropriate for the detection of receptors in the NL, we failed to detect immunoreactivity for group III mGluRs as mentioned above. Accordingly, in the following experiments, we focused on the functional aspects of group II mGluRs.

Metabotropic glutamate receptors are activated constitutively

By using a specific antagonist of group II mGluRs LY341495 (0.2 μM) we tested whether mGluRs are activated constitutively in the low-CF NL neurons. The EPSC amplitude was increased after application of the

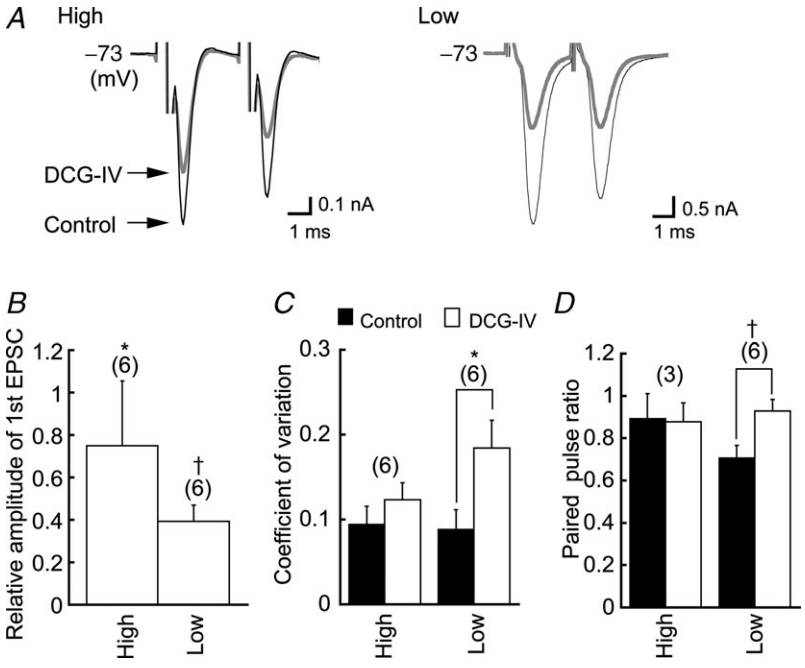

Figure 5. DCG-IV reduces the amplitude of EPSCs
A, DCG-IV (5 μM) reduced the amplitude of EPSCs in high and low-CF neurons (black trace, control; grey trace, DCG-IV). *B*, first EPSC amplitudes of the pair, relative to the control, in DCG-IV. *C* and *D*, coefficient of variation of the first EPSC amplitudes and paired pulse ratio increased significantly in DCG-IV in the low-CF neurons but not in the high-CF neurons. CF, characteristic frequency; DCG-IV, (2*S*,2′*R*,3′*R*)-2-(2′,3′dicarboxycyclopropyl) glycine; EPSC, excitatory postsynaptic current. †$P < 0.01$.

antagonist. Figure 6*A* shows a pair of EPSCs evoked at a 10 ms interval, and the amplitude of the first EPSC was increased by LY341495; 2.11 ± 0.49 nA in the control and 2.51 ± 0.55 nA in LY341495 ($n = 6$, $P < 0.01$; Fig. 6*A* and *B*), while the PPR was reduced (0.83 ± 0.05 in the control and 0.73 ± 0.06 in LY341495, $n = 6$, $P < 0.05$; Fig. 6*C*). Under a train of stimulation, EPSC depression was accelerated by application of LY341495 (Fig. 6*D*). The time constant of depression was 21.31 ± 3.18 ms in the control and 17.32 ± 2.56 ms in LY341495 ($n = 6$, $P < 0.01$), and the relative amplitude of the 10th to the first EPSC was reduced from 0.40 ± 0.01 in the control to 0.32 ± 0.07 in LY341495 ($n = 6$, $P < 0.05$; Fig. 6*F*). Similar results were obtained with EPSPs (Fig. 7). Thus, mGluRs are likely activated constitutively and may contribute to maintain the appropriate size of EPSPs and the sharpness of CD during ongoing sound stimuli.

Activation of metabotropic glutamate receptors by DCG-IV improves coincidence detection

High expression levels of mGluR2/3 in the low-CF neurons might affect the sharpness of CD in NL neurons. DCG-IV (1 μM) reduced the amplitude of EPSP by a factor of 0.58 in the low-CF NL neurons ($n = 7$, $P < 0.01$) (Fig. 8*A* and *B*), while the time course of EPSPs was not altered significantly; the half amplitude width was 1.15 ± 0.25 ms and 1.23 ± 0.25 ms ($n = 7$, $P > 0.40$) in the control and DCG-IV, respectively. In Fig. 5, 5 μM DCG-IV was used to suppress EPSCs to 39% of the control in the low-CF NL neurons (Table 1); however, EPSP amplitude was suppressed even by 1 μM to 58% of the control. We therefore adopted this concentration of DCG-IV in the following experiments to assure neurons to fire in coincidence of bilateral EPSPs. Coincidence of bilateral EPSPs generated action potentials both in the control and in DCG-IV (Fig. 8*C*; $\Delta t = 0$). Firing probability was not largely affected in the control even when a small time difference was placed between bilateral stimuli (Fig. 8*Ca*); however, in DCG-IV, spikes failed more frequently, and this failure progressively increased with time difference (0.4, 0.8 ms; Fig. 8*Cb*). Figure 8*D* summarizes the firing probability measured in four neurons, and DCG-IV reduced the firing probability significantly when Δt was larger than 0.6 ms ($P < 0.05$). Moreover, the reduction of firing probability with the increase in time difference was enhanced in DCG-IV; the slope (Δfiring probability/Δt) was maximum at Δt of 0.5 ms and increased from 0.53 ms^{-1} (control) to

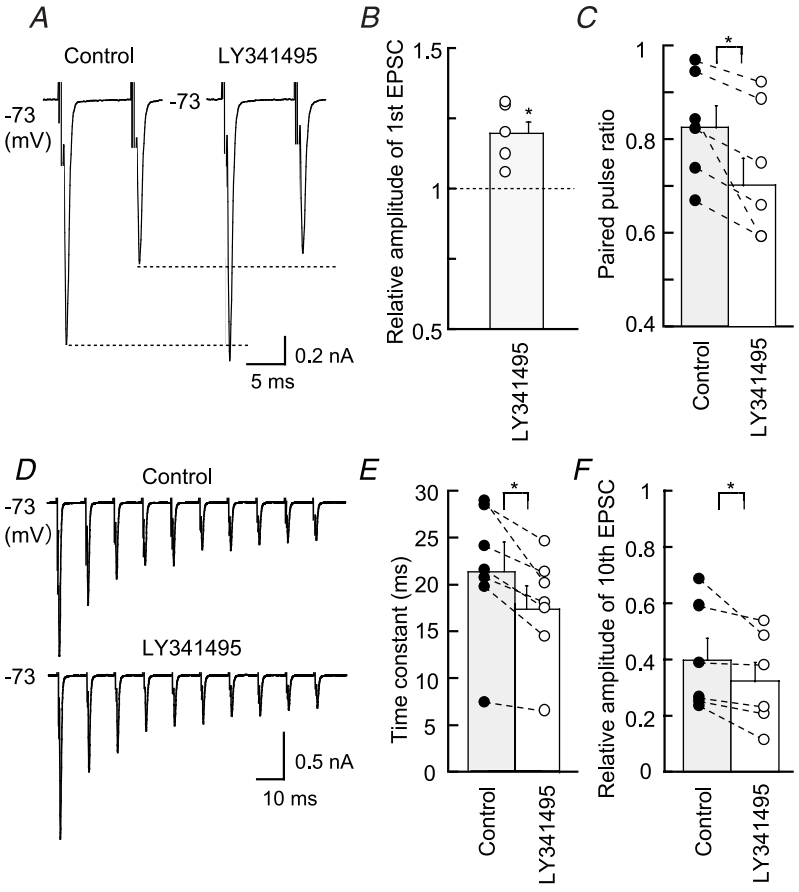

Figure 6. mGluRs are activated constitutively
A, LY341495 (0.2 μM, group II mGluR antagonists) increased the first EPSC of the pair but reduced the second EPSC. Broken lines show the level of the first and second EPSCs in the control. *B* and *C*, size of the first EPSC amplitude was increased by LY341495 (0.2 μM), while the paired pulse ratio (10 ms) was decreased. *D*, EPSCs generated by a train of 10 pulses at 100 Hz (ensemble averages of nine to 11 consecutive traces). *E*, time constant of EPSC depression during a stimulus trains was measured by fitting a single exponential function. *F*, the relative amplitude of the 10th EPSC was reduced significantly by LY341495. *B*, *C*, *E* and *F* are from six neurons. EPSC, excitatory postsynaptic current. *$P < 0.05$.

1.44 ms^{-1} (DCG-IV). Thus, activation of mGluR2/3 could improve the CD of NL neurons.

Discussion

In this study, we found the following: (1) The activation of mGluRs reduced transmitter release by a presynaptic mechanism (Figs 1 and 2). The reduction of transmitter release reduced the depression of EPSC amplitude during a train of stimuli. (2) The expression of mGluR2/3 (group II) was graded along the tonotopic axis in the NL, and the expression was stronger toward the low-CF region of the nucleus (Fig. 3). Specific agonists DCG-IV (group II) and L-AP4 (group III) reduced EPSC amplitude by presynaptic mechanisms (Fig. 5, Table 1). (3) mGluRs are likely activated and may reduce transmitter release constitutively (Figs 6 and 7). (4) Activation of mGluRs improved the sharpness of CD (Fig. 8). These observations indicate that mGluRs might optimize the size of EPSPs and improve the CD in the NL particularly during ongoing stimuli *in vivo*.

However, these observations are not consistent with the absence of effects of mGluRs in the NL of chicken embryo (Tang *et al.* 2009). This lack of effect was likely a consequence of the low expression level of mGluRs in the NL of embryonic chicken (Fig. 4). Consistently, neuronal responsiveness changed greatly after the chicken hatched (Brenowitz & Trussell, 2001; Kuba *et al.* 2002*a*,*b*).

Effects of graded expression of metabotropic glutamate receptors along the tonotopic axis

The accuracy of CD is different among the neurons of three CF regions of NL; accuracy is most precise in the neuron of middle-CF, closely followed by neurons of high-CF and reduced in neurons of low-CF. These differences are largely dependent on the expression level of the Kv1.2 channel, which is responsible for the low-threshold K^+ current (Kuba *et al.* 2005). The Kv1.2 channel is strongly expressed in the middle-CF neurons, accelerates the decay phase of EPSPs and improves CD (Kuba *et al.* 2005). Hyperpolarization-activated and cyclic nucleotide-gated (HCN) channels are other major channels activated at the resting membrane potential in NL neurons. Both HCN1 and HCN2 channels are expressed in NL neurons, and they likely decrease the amplitude and accelerate the time course of EPSPs (Yamada *et al.* 2005). Moreover, HCN2 channels are expressed at a relatively high density in the high-CF NL neurons, and their sensitivity to intracellular

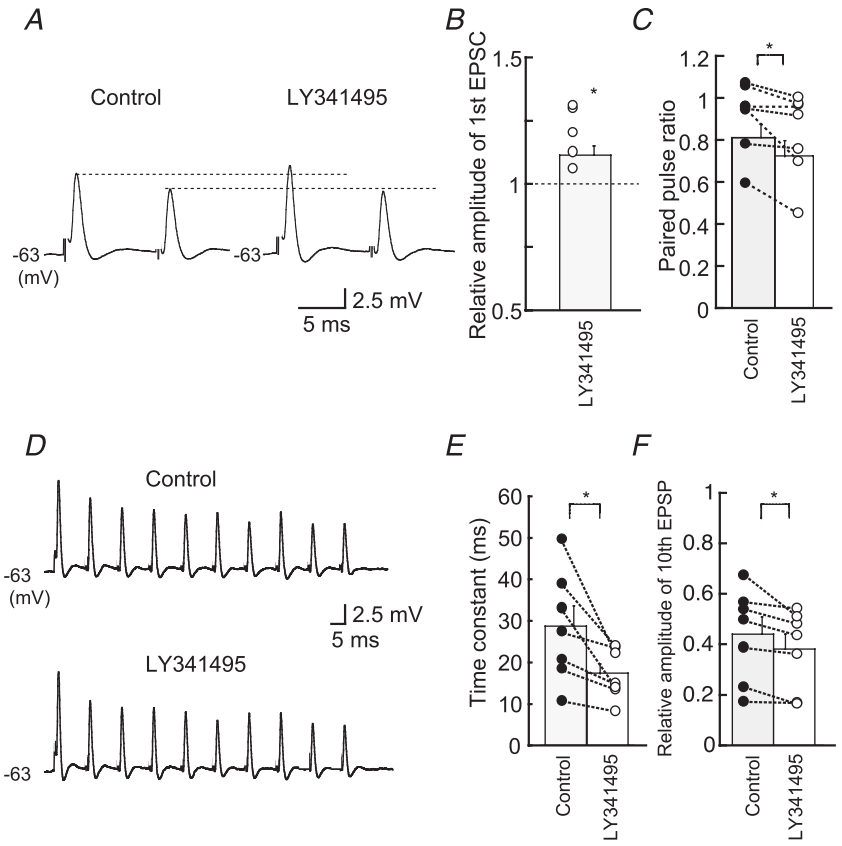

Figure 7. Effects of the mGluR antagonist LY341495 on EPSPs (*A* and *B*)
LY341495 increased the amplitude of first EPSP during the pair of stimuli. Broken lines show the level of the first and second EPSPs from the control. QX314 (5 mM) was included in the internal medium. (*C*) LY341495 reduced the paired pulse ratio significantly. *D*–*F*, EPSP amplitude was reduced more strongly in LY341495 during a train of stimulation. *B*, *C*, *E* and *F* are from seven neurons. EPSP, excitatory postsynaptic potential.

cAMP might have a role in modulating CD in the high-CF NL neurons (Yamada *et al.* 2005).

In this study, we showed that expression of mGluRs is higher in low-CF NL neurons, and activation of mGluRs decreased the EPSP amplitude through presynaptic mechanisms. The small EPSPs may need to be summed to reach threshold in postsynaptic NL neurons, which would reduce the temporal jitter of input spikes; this phenomenon has been demonstrated in the synapse between auditory nerve fibres and low-CF NM neurons in the chicken (Fukui *et al.* 2006) and in the anteroventral cochlear nucleus in cats (Joris *et al.* 1994). Inactivation of Na^+ channels may progress during the temporal summation of EPSPs (Kuba & Ohmori, 2009), which could be compensated for by the rich expression of Na^+ channels in the initial segment of the axon of low-CF NL neurons (Kuba *et al.* 2006). Therefore, CD in the NL may be optimized across CF regions through the cooperation of a variety of pre- and postsynaptic ionic channels and receptors.

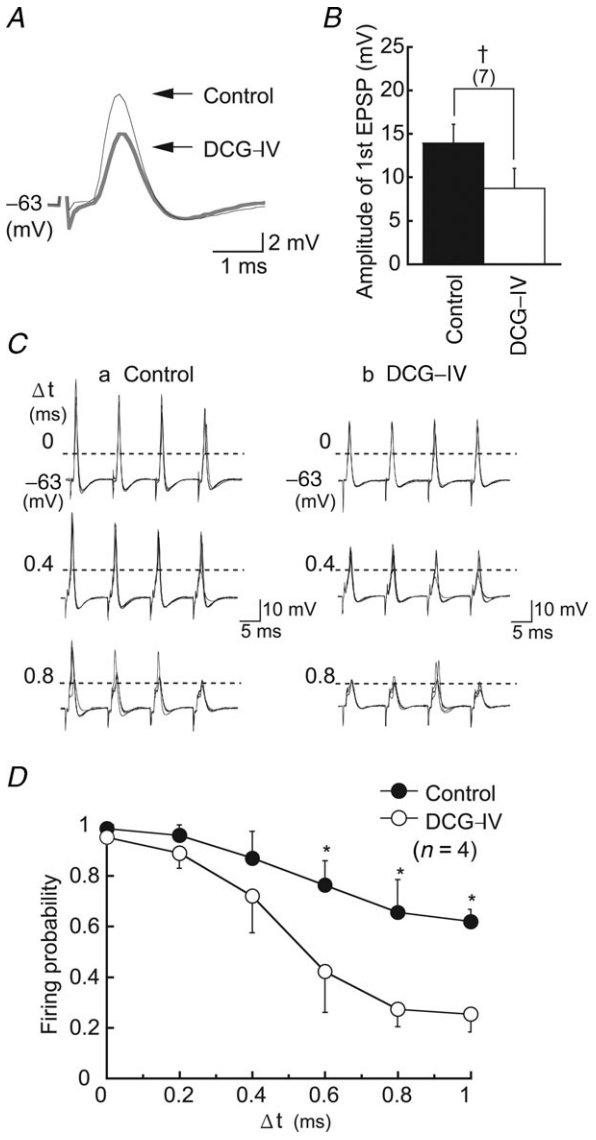

Figure 8. Activation of mGluRs improved coincidence detection
A, DCG-IV (1 μM) reduced the amplitude of EPSP in low-CF neurons (black trace, control; grey trace, DCG-IV). *B*, first EPSP amplitudes in the stimulus train in the control and in DCG-IV ($n = 7$). *C*, spikes generated by coincidence of bilateral stimuli at three different time separations between two sides (Δt) in the control (*Ca*) and in DCG-IV (*Cb*). Spikes were identified by the time derivative of traces. Horizontal broken lines indicate spike thresholds. *D*, probability of spike generation plotted against Δt. DCG-IV reduced the firing probabilities significantly at Δt greater than 0.6 ms. DCG-IV, (2*S*,2′*R*,3′*R*)-2-(2′,3′dicarboxycyclopropyl) glycine; EPSP, excitatory postsynaptic potential.

Expression and activity of metabotropic glutamate receptors in auditory neurons

mGluRs are classified into three subgroups and expressed throughout the brain (Kim *et al.* 2008). Group I mGluRs are located in the postsynaptic membrane and inhibit the Ca^{2+}-dependent release of glutamate by retrograde mechanisms (Kushmerick *et al.* 2004), while group II/III receptors are located in the presynaptic terminals (Barnes-Davies & Forsythe, 1995; Ferraguti & Shigemoto, 2006). In the calyx of Held synapse on MNTB neurons, all three subgroups are expressed. However, DCG-IV (3 μM, a group II mGluR agonist) had no effect on presynaptic Ca^{2+} current, while L-AP4 (50–100 μM, a group III mGluR agonist) suppressed the presynaptic Ca^{2+} current and depressed transmitter release by 80% in the calyx of Held (Takahashi *et al.* 1996). Furthermore, activities of mGluRs are downregulated to compensate for glutamate clearance during development in the calyx of Held synapses (Renden *et al.* 2005). Immunohistochemical evidence suggests an increase in expression of mGluR2/3 in the MNTB synapses in adult rats (Elezgarai *et al.* 2001); however, the functional roles of this increase have yet to be elucidated. The activities of mGluRs were increased with development in the NM-NL synapses of post-hatch chickens, which might have a role in preventing the depletion of synaptic transmission and maintaining CD during ongoing sound. These observations may indicate a functional significance of mGluRs' activities in the mature auditory synapse, despite species differences in the expression and effect of mGluRs.

Metabotropic glutamate receptors regulate synaptic transmission to optimize coincidence detection

Recent *in vivo* recordings from mouse MNTB demonstrated that EPSPs are relatively stable in size, in contrast to extensive short-term depression found in slice preparations (Lorteije *et al.* 2009); this suggests that the release probability of calyx of Held synapses is maintained

at a lower level *in vivo* than in slices. In addition, in rat MNTB neurons, EPSC size changed little during high-frequency stimulation. It was elucidated that EPSC size was maintained stable by the activation of endogenous group III mGluR, which makes the release probability low while it increases the readily releasable pool size and makes the net EPSC unchanged (Billups *et al.* 2005). Our finding of the constitutive activation of mGluRs on the NL synapse may have similar roles on the quantal content in the NM-NL synapse *in vivo*, and may ensure the synaptic transmission to improve CD.

Controls of synaptic transmission by mGluRs were also found in the inhibitory synapse in NL, and there seem to be strong cooperative mechanisms between the excitatory and inhibitory synapses, which control the balance of synaptic inputs and optimize ITD processing in NL. The role of inhibitory synapses is known to improve CD acuity in NL neurons (Funabiki *et al.* 1998; Tang *et al.* 2011). Moreover, GABA transmission to NL neurons is modulated not only through $GABA_B$ receptors but also through mGluRs (Tang *et al.* 2009) and suppressive effects of group II mGluRs emerged in the late phase of development after E15 (Tang & Lu, 2012). Thus, both $GABA_B$ receptor and mGluR activities may control synaptic transmission and have roles in optimizing CD in NL neurons.

References

Barnes-Davies M & Forsythe ID (1995). Pre-and postsynaptic glutamate receptors at a giant excitatory synapse in rat auditory brainstem slices. *J Physiol* **488**, 387–406.

Billups B, Graham BP, Wong AY & Forsythe ID (2005). Unmasking group III metabotropic glutamate autoreceptor function at excitatory synapses in the rat CNS. *J Physiol* **565**, 885–896.

Brenowitz S & Trussell LO (2001). Maturation of synaptic transmission at end-bulb synapses of the cochlear nucleus. *J Neurosci* **21**, 9487–9498.

Carr CE & Konishi M (1990). A circuit for detection of interaural time differences in the brain stem of the barn owl. *J Neurosci* **10**, 3227–3246.

Conn PJ & Pin JP (1997). Pharmacological and functions of metabotropic glutamate receptors. *Annu Rev Pharmacol Toxicol* **37**, 205–237.

Cook DL, Schwindt PC, Grande LA & Spain WJ (2003). Synaptic depression in the localization of sound. *Nature* **421**, 66–70.

Corti C, Restituito S, Rimland JM, Brabet I, Corsi M, Pin JP & Ferraguti F (1998). Cloning and characterization of alternative mRNA forms for the rat metabotropic glutamate receptors mGluR7 and mGluR8. *Eur J Neurosci* **10**, 3629–3641.

Corti C, Aldegheri L, Somogyi P & Ferraguti F (2002). Distribution and synaptic localisation of the metabotropic glutamate receptor 4 (mGluR4) in the rodent CNS. *Neuroscience* **110**, 403–420.

Elezgarai I, Bilbao A, Mateos JM, Azkue JJ, Benítez R, Osorio A, Díez J, Puente N, Doñate-Oliver F & Grandes P (2001). Group II metabotropic glutamate receptors are differentially expressed in the medial nucleus of the trapezoid body in the developing and adult rat. *Neuroscience* **104**, 487–498.

Ferraguti F & Shigemoto R (2006). Metabotropic glutamate receptors. *Cell Tissue Res* **326**, 483–504.

Fukui I, Sato T & Ohmori H (2006). Improvement of phase information at low sound frequency in nucleus magnocellularis of the chick. *J Neurophysiol* **96**, 633–641.

Funabiki K, Koyano K & Ohmori H (1998). The role of GABAergic inputs for coincidence detection in the neurones of nucleus laminaris of the chick. *J Physiol* **508**, 851–869.

Joris PX, Carney LH, Smith PH & Yin TC (1994). Enhancement of neural synchronization in the anteroventral cochlear nucleus. I. Responses to tones at the characteristic frequency. *J Neurosci* **71**, 1022–1036.

Joseph AW & Hyson RL (1993). Coincidence detection by binaural neurons in the chick brain stem. *J Neurophysiol* **69**, 1197–1211.

Kim CH, Lee J, Lee JY & Roche KW (2008). Metabotropic glutamate receptors: phosphorylation and receptor signalling. *J Neurosci Res* **86**, 1–10.

Klumpp RG & Eady HR (1956). Some measurements of interaural time difference thresholds. *J Acoust Soc Am* **28**, 859–860.

Korn H & Faber DS (1991). Quantal analysis and synaptic efficacy in the CNS. *Trends Neurosci* **14**, 439–445.

Kuba H, Koyano K & Ohmori H (2002*a*). Synaptic depression improves coincidence detection in the nucleus laminaris in brainstem slices of the chick embryo. *Eur J Neurosci* **15**, 984–990.

Kuba H, Koyano K & Ohmori H (2002*b*). Development of membrane conductance improves coincidence detection in the nucleus laminaris of the chicken. *J Physiol* **540**, 529–542.

Kuba H, Yamada R & Ohmori H (2003). Evaluation of the limiting acuity of coincidence detection in nucleus laminaris of the chicken. *J Physiol* **552**, 611–620.

Kuba H, Yamada R, Fukui I & Ohmori H (2005). Tonotopic specialization of auditory coincidence detection in nucleus laminaris of the chick. *J Neurosci* **25**, 1924–1934.

Kuba H, Ishii TM & Ohmori H (2006). Axonal site of spike initiation enhances auditory coincidence detection. *Nature* **444**, 1069–1072.

Kuba H & Ohmori H (2009). Roles of axonal sodium channels in precise auditory time coding at nucleus magnocellularis of the chick. *J Physiol* **587**, 87–100.

Kushmerick C, Price GD, Taschenberger H, Puente N, Renden R, Wadiche JI, Duvoisin RM, Grandes P & von Gersdorff H (2004). Retroinhibition of presynaptic Ca^{2+} currents by endocannabinoids released via postsynaptic mGluR activation at a calyx synapse. *J Neurosci* **24**, 5955–5965.

Lachica EA, Rübsamen R, Zirpel L & Rubel EW (1995). Glutamatergic inhibition of voltage-operated calcium channels in the avian cochlear nucleus. *J Neurosci* **15**, 1724–1734.

Leão RM & von Gersdorff H (2002). Noradrenaline increases high-frequency firing at the calyx of Held synapse during development by inhibiting glutamate release. *J Neurophysiol* **87**, 2237–2306.

Lorteije JA, Rusu SI, Kushmerick C & Borst JG (2009). Reliability and precision of the mouse calyx of Held synapse. *J Neurophysiol* **29**, 13770–13784.

Lu Y (2007). Endogenous mGluR activity suppresses GABAergic transmission in avian cochlear nucleus magnocellularis neurons. *J Neurophysiol* **97**, 1018–1029.

Maki AA, Beck MM, Gleaves EW & De Shazer JA (1990). CSF ion composition and manipulation during thermoregulation in an avian species, *Gallus domesticus*. *Comp Biochem Physiol A Comp Physiol* **96**, 135–140.

Manabe T, Wyllie DJ, Perkel DJ & Nicoll RA (1993). Modulation of synaptic transmission and long-term potentiation: effects on paired pulse facilitation and EPSC variance in the CA1 region of the hippocampus. *J Neurophysiol* **70**, 1451–1459.

Nakajima Y, Iwakabe H, Akazawa C, Nawa H, Shigemoto R, Mizuno N & Nakanishi S (1993). Molecular characterization of a novel retinal metabotropic glutamate receptor mGluR6 with a high agonist selectivity for L-2-amino-4-phosphonobutyrate. *J Biol Chem* **268**, 11868–11873.

Nishimaki T, Jang IS, Ishibashi H, Yamaguchi J & Nabekura J (2007). Reduction of metabotropic glutamate receptor-mediated heterosynaptic inhibition of developing MNTB-LSO inhibitory synapses. *Eur J Neurosci* **26**, 323–330.

Otis TS & Trussell LO (1996). Inhibition of transmitter release shortens the duration of the excitatory synaptic current at a calyceal synapse. *J Neurophysiol* **76**, 3584–3588.

Parks TN & Rubel EW (1975). Organization and development of the brain stem auditory nuclei of the chicken: organization of projections from n. magnocellularis to n. laminaris. *J Comp Neurol* **164**, 435–448.

Phillips T, Makoff A, Murrison E, Mimmack M, Waldvogel H, Faull R, Rees S & Emson P (1998). Immunohistochemical localisation of mGluR7 protein in the rodent and human cerebellar cortex using subtype specific antibodies. *Brain Res Mol Brain Res* **1**, 132–141.

Renden R, Taschenberger H, Puente N, Rusakov DA, Duvoisin R, Wang LY, Lehre KP & von Gersdorff H (2005). Glutamate transporter studies reveal the pruning of metabotropic glutamate receptors and absence of AMPA receptor desensitization at mature calyx of Held synapses. *J Neurosci* **14**, 8482–8497.

Reyes AD, Rubel EW & Spain WJ (1996). In vitro analysis of optimal stimuli for phase-locking and time-delayed modulation of firing in avian nucleus laminaris. *J Neurosci* **16**, 993–1007.

Rubel EW & Parks TN (1975). Organization and development of the brain stem auditory nuclei of the chicken: tonotopic organization of n. magnocellularis and n. laminaris. *J Comp Neurol* **164**, 411–434.

Takahashi T, Forsythe ID, Tsujimoto T, Barnes-Davies M & Onodera K (1996). Presynaptic calcium current modulation by a metabotropic glutamate receptor. *Science* **274**, 594–597.

Takahashi T, Kajikawa Y & Tsujimoto T (1998). G-Protein-coupled modulation of presynaptic calcium currents and transmitter release by a GABAB receptor. *J Neurosci* **18**, 3138–3146.

Tang ZQ, Gao H & Lu Y (2009). Control of a depolarizing GABAergic input in an auditory coincidence detection circuit. *J Neurophysiol* **102**, 1672–1683.

Tang ZQ, Dinh EH, Shi W & Lu Y (2011). Ambient GABA-activated tonic inhibition sharpens auditory coincidence detection via a depolarizing shunting mechanism. *J Neurosci* **16**, 6121–6131.

Tang ZQ & Lu Y (2012). Development of GPCR modulation of GABAergic transmission in chicken nucleus laminaris neurons. *PLoS ONE* **7**, e35831.

von Gersdorff H, Schneggenburger R, Weis S & Neher E (1997). Presynaptic depression at a calyx synapses: the small contribution of metabotropic glutamate receptors. *J Neurosci* **17**, 8137–8146.

Wada K, Sakaguchi H, Jarvis ED & Hagiwara M (2004). Differential expression of glutamate receptors in avian neural pathways for learned vocalization. *J Comp Neurol* **476**, 44–64.

Yamada R, Kuba H, Ishii TM & Ohmori H (2005). Hyperpolarization-activated cyclic nucleotide-gated cation channels regulate auditory coincidence detection in nucleus laminaris of the chick. *J Neurosci* **25**, 8867–8877.

Yin TCT & Chan JCK (1990). Interaural time sensitivity in medial superior olive of cat. *J Neurophysiol* **64**, 465–488.

Zhang S & Trussell LO (1994). Voltage clamp analysis of excitatory synaptic transmission in the avian nucleus magnocellularis. *J Physiol* **480**, 123–136.

Author contributions

Conception and design of the experiments: H.K. and H.O. Collection, analysis and interpretation of data: H.O. and R.Y. Drafting and revising the article for important intellectual content: H.O., R.Y., H.K. and H.O. All authors approved the final version.

Acknowledgements

We appreciate Mr M. Fukao's work machining the equipment. This study was supported by Grants-in-Aid from MEXT to R.Y. (no. 21700431), H.K. (no. 22680031), and H.O. (no. 20220008) and the JST PRESTO program to H.K.

Translational perspective

Interaural time difference (ITD) is a major cue for localizing a sound source. ITD depends on the head size of animal and is generally extremely small. In birds, ITD is processed in the nucleus laminaris (NL), where a spike is generated in coincidence of ipsilateral and contralateral excitatory postsynaptic potentials (EPSPs; coincidence detection, CD). Fast and small EPSPs are known to improve the accuracy of CD. The EPSP time course was accelerated by a variety of postsynaptic factors, and the size decreases during a train of stimulation due to synaptic depression. However, EPSPs fail to trigger spikes and abort CD when they become too small. Therefore, some regulatory mechanism is required to optimize EPSP size. Metabotropic glutamate receptors (mGluRs) are known to regulate transmitter release in a variety of synapses. We found that activation of presynaptic mGluRs reduced EPSP size but improved CD. Thus, presynaptic mGluRs may operate as a self-regulatory mechanism to optimize EPSP size and may have roles in maintaining the accuracy of CD, particularly during ongoing stimuli.